



Tanzania Journal of Science 46(2): 241-253, 2020

ISSN 0856-1761, e-ISSN 2507-7961

© College of Natural and Applied Sciences, University of Dar es Salaam, 2020

The Geochemical Compositions and Origin of Sand Dunes in the Olduvai Gorge–Eastern Serengeti Plains, Northern Tanzania

Dalaly P Kafumu

Earth Sciences Institute of Shinyanga, Ndala, Shinyanga, Plot No. 91, Block HH,

P. O. Box 1016, Shinyanga, Tanzania.

E-mail: pdkafumu@gmail.com

Received 24 January 2020, Revised 14 April 2020, Accepted 27 April 2020, Published June 2020

Abstract

This paper reports the composition and origin of black sand dunes that occur in the eastern Serengeti plains near the Olduvai Gorge hominid site in Tanzania. Grain size analysis reflected light microscopic examination, and scanning electron microscopy (SEM) analysis identified very fine to coarse sand fraction mineral grains of between 0.065 mm and 1 mm, composed of augite, fassaite and omphacite pyroxenes; garnet and sillimanite silicate mineral grains. The pyroxene minerals (augite, omphacite and fassaite) constitute 95.4% by volume of the sand dunes. The other mineral grains are silicate minerals that include garnet and sillimanite, together form the remaining 4.6% by volume. Major and trace elements of the sand dunes as analyzed by inductively coupled plasma – atomic emission spectrometer (ICP-AES) show natro-carbonatite geochemistry of up to 7.38wt.% Na₂O and 5.0wt.% CaO. Also the sand dunes are rich in SiO₂ (47.37wt.%), Al₂O₃ (11.22wt.%), Fe₂O₃ (12.51wt.%) and MgO (8.45wt.%). Trace elements include 15.20 ppm Cu, 17.90 ppm Co, 146.7 ppm Zn, 121.20 ppm Cr and 29.30 ppm Ni. This geochemical composition of the Olduvai Gorge sand dunes resembles the composition of volcanic rocks from Oldoinyo Lengai volcanic eruption; suggesting that the sand dunes originated from the Holocene Oldoinyo Lengai volcanism located about 100 km east of the area.

Keywords: Geochemical analysis; major elements; Oldoinyo Lengai; Olduvai Gorge; pyroxenes; trace elements

Introduction

Black sand dunes that occur in the eastern Serengeti Plain near the Olduvai Gorge hominid site within the Ngorongoro Conservation Area Authority in Tanzania are identified as volcanic sand dunes (Hay 1976). The sand dunes are consistently blown by a west-easterly wind and migrate towards the west. The sand dunes have been named “shifting sands” as they move from east to west across the plains. It is estimated that these shifting sand dunes have been moving for 3 thousand years at a rate of between 15 and 20 m per year (Hanby and Bygott 1998, Africantourer 2020). Most of the dunes have spread over the plains, but there are still

several dunes of approximately 10 m high and 60 m wide that continue to spread westward across the plains (Figure 1). The geochemistry of the sand dunes has not been studied, and this is the first study to look into their compositions and origin.

The sand dunes are situated within latitudes 2°52' S to 2°57' S and longitudes 35°16' E to 35° 20' E in the Eyasi Rift graben of the Great East African Rift System (Figure 2). The area is a vast flat lowland plain with an altitude of 1,800 m above sea level in contrast to the 3,000 m above sea level towering Ngorongoro Highlands to the east of the area and the 2,300 m above sea level Oldoinyo Olgol mountains to the north.

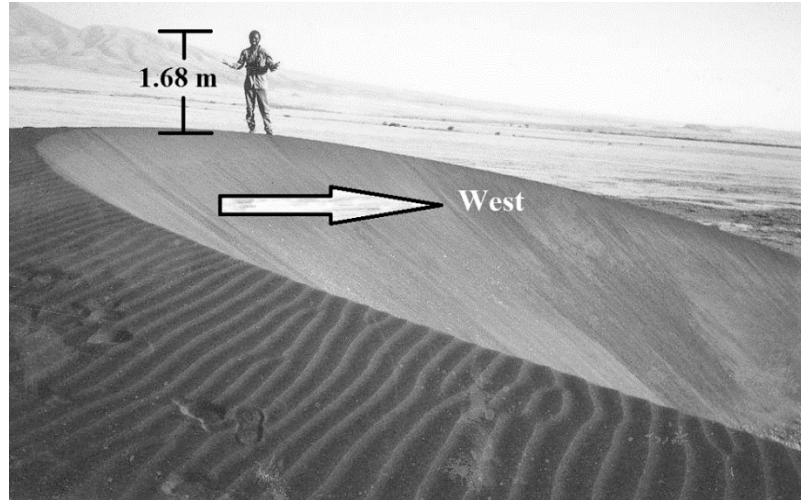


Figure 1: 10 m high and 60 m wide black sand dunes that continue to spread westward. (The arrow indicates the direction of the sand dunes movement across the Serengeti Plains. The scale of the picture is indicated by the person standing on the dune who is 1.68 m tall).

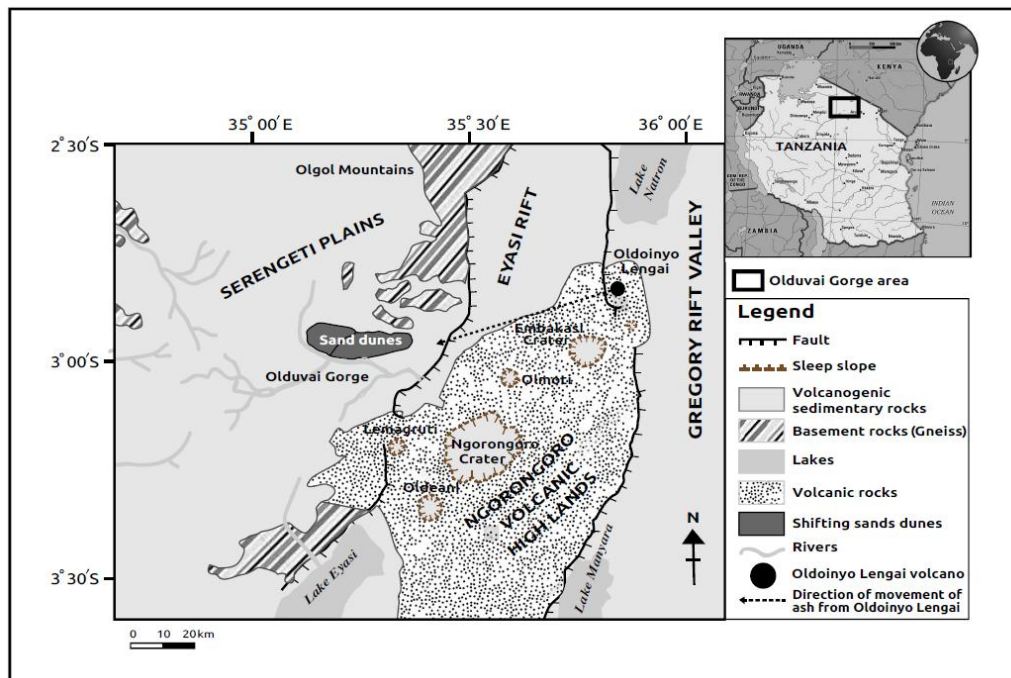


Figure 2: The geological map of the Olduvai Gorge area [Note the position of Oldoinyo Lengai volcano, the direction of ashes travel and location of the sand dunes] (Modified after: Hay 1976, Kafumu 2000).

Geological setting and background

The geological setting of the area is characterized by a stratigraphy (Figure 3) that begins with the Precambrian rock basement, outcropping mainly in the north eastern part of the area. These Precambrian rocks that are composed of mainly gneiss were mapped as inselbergs north of the Olduvai Gorge and in the Olgoidjo and Agata Kiti hills. The inselbergs are part of the Mozambique Belt quartzite and mica schist dated between 500 and 800 Ma old (Roger 2018). The Olgol Mountains mapped in the north of the area (Figure 2) also represent Precambrian rocks. Mapping also indicated that Neogene volcanic rocks uncomfortably overlie the Precambrian basement rocks. Quaternary volcanogenic-sedimentary rocks and sediments lay uncomfortably on Neogene volcanic rocks. Finally, the volcanogenic-sedimentary units are covered by Olbabal alluvium and the rest of the area is covered by either white calcareous tuffs or black volcanic sands (Hay 1968, Hay 1976, Kafumu 2000, Figure 2).

These volcanogenic-sedimentary units were laid down either in shallow paleolakes as sands, clays or reworked pyroclasts (Hay 1976). Detailed mapping of the composition of volcano-sedimentary units in the study area showed that they contain tuffs, lava flows and clayey to silty-sandy units. These units also contain numerous paleosol levels (Kafumu 2000, Ashley and Driese 2000, Beverly et al. 2017) that are dwelling places of hominids like the *Australopithecus (Paranthropus) boisei* (Leakey and Roe 1995).

The rifting phase in this area was activated in the Miocene about 15 Ma (Shackleton 1978) though studies by Macheyeki (2008) and Nyblade and Brazier (2002) indicate that rifting propagated towards the northern part of Tanzania (from Kenya) around 12 Ma to 10 Ma. It then formed the Pleistocene Serengeti paleo-lake basin (Shackleton 1978). The basin started to be filled with sedimentary sediments

intercalated with volcanic tephra (Pickering 1994). About 100 m thick volcanogenic-sedimentary units were laid down on a pre-existing Precambrian basement floor (Figure 3). In times of retreated lake shores, paleosols were formed during landscape stability when pedogenesis took place and where animals and plant life could thrive (Kafumu 2000, Ashley and Driese 2000, Beverly et al. 2017). The sediment accumulation culminated with a pouring of black ashes and sands about 12,000 BP to cover the eastern Serengeti Plain (Pickering 1994). The Olduvai George began to form (cutting through the sediments) about 10,000 BP (Pickering 1994).

The stratigraphy of the Olduvai Gorge hominid site (Figure 3) is therefore a series of volcanogenic-sedimentary rocks composed of mixed lacustrine-fluviatile clayey to silty-sands units in alternation with paleosols, volcanic tuffs and reworked pyroclasts within distinct recognizable Bed I, Bed II, Bed III, Bed IV and Bed V (Hay 1968, 1976, Kafumu 2000) laying on Neogene volcanic lava flows. The sequences rest unconformably on gneissose metamorphic rocks of Precambrian age.

Materials and Methods

The methods employed were field geological mapping to describe the geological setting of the area and sand dune sampling for laboratory analyses and examinations. Laboratory methods included grain size analysis, reflected light microscopy, inductively coupled plasma-atomic emission spectrometry (ICP-AES), and scanning electron microscopy (SEM).

Ten portions of 500 g weight each were obtained from five different dunes at the rear and lee sides of the dunes. These samples were dried, mixed and homogenized into one 5 kg bulk sample. A grain size analysis was performed on a 4.5 kg sand sample to obtain average grain sizes. The remaining 500 g sample was split into four equal samples each weighing 125 g. One 125 g sample portion was examined by a reflected light microscope

to determine the shape, size and proportions of each type of mineral grains.

The other 125 g sample was crushed, powdered and then a 0.1 to 0.2 g sample was obtained and dissolved into solution according to the standard dissolution methods of Potts (1987) and Dean (2005) by mixing the sample with 0.4 g of lithium metaborate (LiBO₂) flux and placed into a Pt-Au crucible. A 10 µL lithium bromide (LiBr) wetting agent was added to the sample and then the mixture fused at 1050 °C for 10 to 12 minutes forming a solid bead at the bottom of the crucible. The bead was cooled

and popped off from the crucible bottom, placed in a beaker and then dissolved in 50 mL of 10% nitric acid (10% HNO₃) solution. The solution was filtered and a final analyte solution was prepared by pipetting a 5-mL aliquot of the filtered solution and diluting it with 35 mL of 10% HNO₃ (to a total of 40 mL). The cool solution was then analysed for major and trace elements by ICP-AES. Few grains from the remaining 125 g sample were examined by SEM analysis for geochemical elements and mineralogical compositions.

DEPTH (m)	STRATA	TYPES OF ROCKS OR SEDIMENTS	CHRONO-STRATIGRAPHY	
0 20 40 60 80	Recent Sediments	Calcareous sands and ash falls	HOLOCENE	QUATERNARY
	Bed V	Alluvium, aeolian sediments, tuffs, silts and sands		
	Bed IV	Volcanogenic-sedimentary rocks (mixed lacustrine-fluviatile clayey to silty-sands sedimentary units in alternation with paleosols, volcanic tuffs and reworked pyroclasts)	PLEISTOCENE	
	Bed III			
	Bed II			
60 80	Bed I	----- Unconformity -----	PLIOCENE	NEOGENE
80	Volcanics	Volcanic Rocks		
80 100		----- Unconformity -----		PRECAMBRIAN
	100	Gneiss		

Figure 3: The stratigraphic column of the Olduvai Gorge area (modified after Hay 1976 and Kafumu 2000).

Results

The sieve grain size analysis revealed that the sands had grain sizes between 0.065 mm and 1 mm (very fine to coarse grained sands). Reflected light microscopic examinations (Figure 4) revealed that the sand dunes were composed of dark coloured prismatic augite, and light coloured omphacite, and fassaite pyroxene mineral grains. Other mineral grains identified were sillimanite and garnet silicate minerals.

Furthermore, reflected light microscopic observations of mineral grain counts (Table 1 and Figure 5) in ten observations revealed that pyroxene mineral grains (augite, omphacite and fassaite) constitute 95.4% by volume of the sand dunes. The remaining small portion (4.6% by volume) is made of silicate mineral grains (garnet and sillimanite).

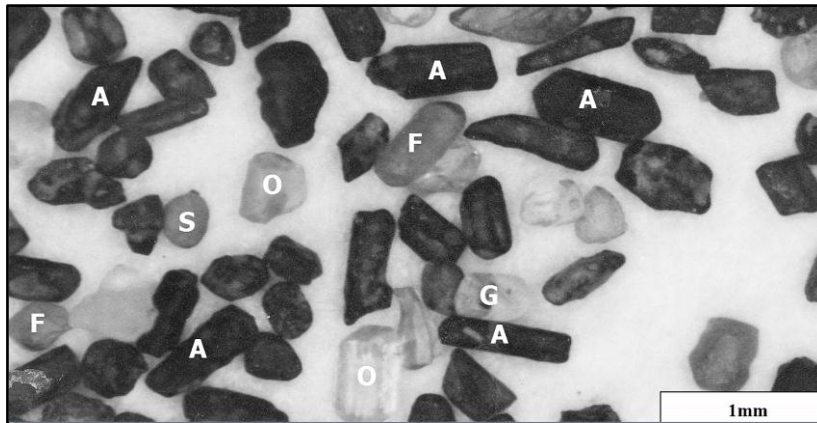


Figure 4: Black sand dune mineral grains from the Olduvai Gorge that are composed of prismatic ferrous black augite pyroxenes (A) and light coloured ferrous omphacite pyroxenes (O), fassaite pyroxenes (F), sillimanite (S) and garnet (G) mineral grains as observed through a reflected light microscope.

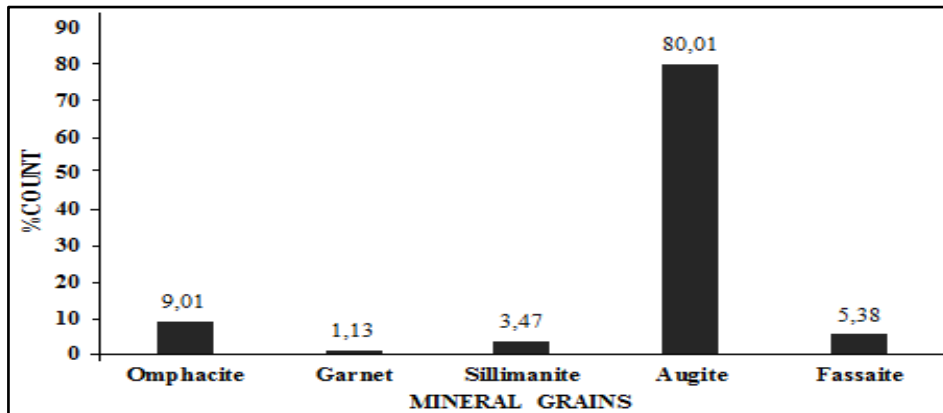


Figure 5. Mineral type distribution by weight obtained from mineral counts in ten observations of the Olduvai Gorge sand dunes: [Omphacite (9.01%), Garnet (1.14%), Sillimanite (3.47%), Augite (81.01%), and Fassaite (5.38%)].

Table 1: Reflected light microscopic examinations of sand dunes: mineral grains counts indicating a variety of pyroxene mineral grains accounting for 95.4% by volume (a+b+c) of the sand dunes; where a = augite (81.01%); b = omphacite (9.01%) and c = fassaite (5.38%). *Other grains are composed of silicate mineral grains that account together for 4.6% by volume (d+e) of the sand dunes; where d = garnet (1.13%) and e = sillimanite (3.47%).

Observations	Total counts	Augite		Omphacite		Fassaite		Garnet*		Sillimanite*	
		Counts	%	Counts	%	Counts	%	Counts	%	Counts	%
1	50	40	80.00	5	10.00	3	6.00	1	2	1	2
2	66	55	83.33	6	9.09	1	1.52	0	0	4	6.06
3	60	49	81.67	6	10.00	1	1.67	2	3.33	2	3.33
4	59	45	76.27	4	6.78	7	11.86	0	0	3	5.09
5	70	55	78.57	6	8.57	4	5.71	2	2.86	3	4.29
6	61	41	67.21	8	13.12	6	9.84	1	1.64	5	8.20
7	51	42	82.35	7	13.73	1	1.96	0	0	1	1.96
8	40	36	90.00	0	0	4	10.00	0	0	0	0
9	66	54	81.82	8	12.12	2	3.03	1	1.51	1	1.51
10	45	40	88.90	3	6.67	1	2.22	0	0	1	2.22
Average total %count		81.01(a)		9.01(b)		5.38(c)		1.13(d)		3.47(e)	

Scanning electron microscopy (Table 2 and Figure 6) analysis of selected grains revealed that the sand dunes are mainly composed of pyroxene silicate mineral grains augite, omphacite and fassaite and a small proportion of other silicates that include sillimanite

mineral grains. The augite and omphacite mineral grains are essentially aluminium silicates rich in iron and calcium; while fassaite mineral grains are devoid of iron and sillimanite mineral grains devoid in both iron and calcium (Figure 6).

Table 2: Scanning Electron Microscopy (SEM) analysis (a summary dataset of the Appendix) of some mineral grains (augite, omphacite, fassaite and sillimanite) of black sand dunes of the Olduvai Gorge in the Serengeti Plains

Elements	Augite		Omphacite		Sillimanite		Fassaite	
	Atom%	Element wt.%	Atom%	Element wt.%	Atom%	Element wt.%	Atom%	Element wt.%
Oxygen	55.25	36.49	52.89	35.86	67.74	54.10	72.40	59.04
Na	0.85	0.80	3.83	3.73	0	0	0.50	0.58
Mg	2.68	2.69	2.83	2.92	0	0.70	2.71	3.36
Al	4.48	4.99	6.32	7.22	1.12	1.51	6.17	8.49
Br	1.91	6.31	0	0	0	0	0	0
Si	23.00	26.67	23.02	27.40	29.50	41.37	14.20	20.33
P	0.67	0.86	0	0	0	0	0.51	0.81
Cl	0.22	0.32	0	0	0	0.20	0.13	0.24
K	1.01	1.64	0.96	1.59	0.30	0.58	0.66	1.31
Ca	5.40	8.94	3.90	6.63	0.36	0.72	2.27	4.63
Ti	0.32	0.62	0.44	0.90	0	0	0.11	0.27
Mn	0.20	0.46	0.18	0.43	0	0	0	0
Fe	4.00	9.21	5.63	13.32	0.30	0.82	0	0

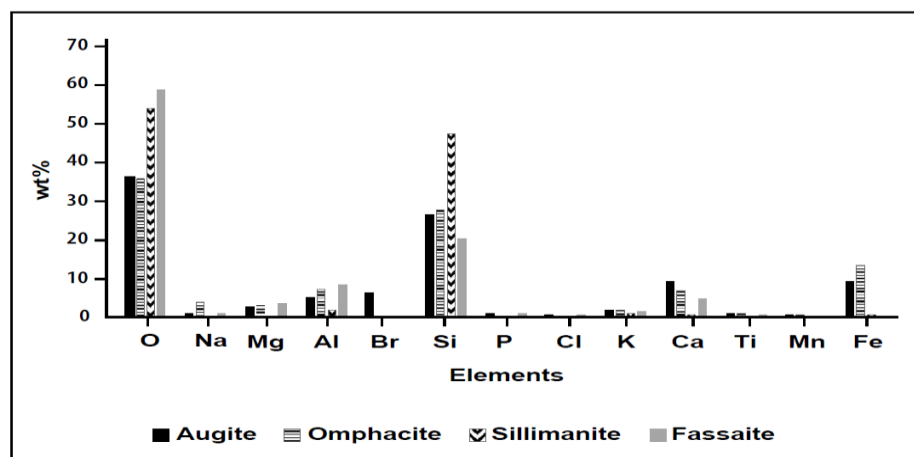


Figure 6: Graphic representation of scanning electron microscopy (SEM) analyses of augite, omphacite, sillimanite and fassaite mineral grains from black sand dunes of the Olduvai Gorge showing proportions of chemical elements in each mineral [aluminum-calcium-sodium-iron silicates].

Major elements geochemistry (Table 3) indicated that the sands are relatively rich in SiO_2 (43.45–47.37 wt.%), Al_2O_3 (1.51–11.22 wt.%), MgO (2.69–8.45 wt.%) and Fe_2O_3 (0.92–12.51 wt.%). The sands have also elevated values of Na_2O (0.58–7.38 wt.%) and CaO (0.72–5.0 wt.%) and high trace

elements (Table 2) of Zn (146.7 ppm), Cr (121.2 ppm) and Ni (29.3 ppm) (Table 4). Table 4 also offers a compositional comparison between the major and trace elements geochemistry of Olduvai Gorge shifting sand dunes and Oldoinyo Lengai volcanic rocks.

Table 3: Major elements (whole rock) geochemical composition of Serengeti Plains shifting sands as compared to the Oldoinyo Lengai volcanic rocks composition (from Bell and Simonetti 1996) display similarities (*n.a. = not analyzed).

Whole rock	Olduvai Gorge sand dunes	Oldoinyo Lengai volcanic rocks (Bell and Simonetti 1996)
	Content (wt.%)	Content (wt.%)
SiO_2	43.45–47.37	43.07–52.9
Al_2O_3	1.51–11.22	1.26–19.83
Na_2O	0.58–7.38	7.21–10.21
K_2O	0.25–0.35 (low)	4.31–5.88
CaO	0.72–5.00	2.88–11.68
MgO	2.69–8.45 (high)	0.52–2.02
Fe_2O_3	0.92–12.51	3.66–7.21
MnO	0.40–0.46	0.17–0.38
TiO_2	0.62–6.85 (high)	0.77–1.21
P_2O_5	0.81–2.09 (high)	0.03–0.57
L.O.I.	1.42	*n.a.

Note: L.O.I = loss of ignition.

Table 4: Trace elements geochemical composition of Serengeti Plains shifting sands as compared to the Oldoinyo Lengai volcanic rocks composition (From Bell and Simonetti 1996) display similarities (*n.a. = not analyzed).

Trace elements	Olduvai Gorge sand dunes	Oldoinyo Lengai volcanic rocks (Bell and Simonetti 1996)
	Content (ppm)	Content (ppm)
Cu	15.20	12.0–47.0
Co	17.90	*n.a.
Zn	146.70	108.0–155.0
Cr	121.20 (high)	<10
Ni	29.30	10.0–50.0

Discussions

The Olduvai Gorge sand dunes reported in this study are composed of 0.065 mm to 1 mm very fine to coarse sand fraction pyroxenes and other silicate mineral grains. This composition is similar to the composition of igneous clinopyroxene xenoliths of the carbonatite volcanics of the Oldoinyo Lengai eruption that were described by Dawson et al. (1995b). The mineral chemistry study of plutonic igneous xenolith from the Oldoinyo Lengai carbonatite volcano by Dawson et al. (1995b) observed 0.2 mm to 1 mm clinopyroxene minerals mainly titaniferrous-augites, mica and olivine in the Oldoinyo Lengai volcanic melt that was dated between 0.00 and 0.022 Ma (Dawson et al 1995a, Žaba and Gaidzik 2011, Mollel and Swisher 2012, Sherrod et al 2013).

Similarly, the geochemical signatures of major elements (SiO_2 , Al_2O_3 , Fe_2O_3 , Na_2O , and CaO) of the sand dunes of the Olduvai Gorge sand dunes are similar to those of the Oldoinyo Lengai volcanic rocks (Table 1, Bell and Simonetti 1996). Furthermore, trace elements contents of the Olduvai Gorge sands Cu (15.20 ppm), Zn (146.70 ppm) and Ni (29.30 ppm) of the sands are also comparable to the values of Cu (12.0–47.0 ppm), Zn (108.0–155.0 ppm) and Ni (10.00–50.0 ppm) found in the Oldoinyo Lengai volcanic eruption (Table 4, Bell and Simonetti 1996).

However, the slightly elevated values of MgO (8.45 wt.%), TiO_2 (6.85 wt.%), P_2O_5 (2.09 wt.%), and Cr (121.20 ppm) in the sand dunes compared to the Oldoinyo Lengai tephra with low values of MgO (0.52–2.02 wt.%); TiO_2 (0.77–1.21 wt.%) and P_2O_5 (0.03–0.57 wt.%) (Table 3, Table 4, Bell and Simonetti 1996) may be due to the weathering and erosion of olivine and mica minerals from the proto sands that came from the Oldoinyo Lengai volcanism, thus concentrating the slightly resistant minerals like pyroxenes that have higher in contents of such elements in the present day sand dunes. Similarly, the reduced values of K_2O (0.25–0.35 wt.%) in the sand dunes (Table 3, Bell and Simonetti 1996) may be due to weathering away of K_2O -rich minerals such as mica from the original sands, thus diluting the K_2O geochemical contents of these elements in the present day sand dunes.

Therefore, the Olduvai Gorge sand dunes reported in this study contain a variety of clinopyroxenes like augite, fassaite and omphacite that form the large part of the sand dunes (~95%) and a small portion made up of silicate minerals like garnet and sillimanite (~5%) all that came from a volcanic source. These sand dunes originated from volcanic rocks in the vicinity and in the cause of sand dune migration, easily weathered minerals from the volcanic rocks were weathered out and the resistant mainly pyroxenes and

silicate minerals remained as main constituents of the sand dunes.

During the Holocene, a tephra fall might have erupted from the Oldoinyo Lengai located about 100 km east of the area and blown by wind landed in the Serengeti Plains (Figure 7) where it was exposed to rolling and weathering. Due to water and wind weathering actions, the freshly erupted tephra were changed in compositions into sand dunes rich in relatively resistant to weathering augite-pyroxenes mineral grains and devoid of easily weatherable olivine and mica mineral grains.

It is prudent to conclude that, although the most common constituents of mature sand dunes in inland continental settings and non-tropical coastal settings contain silica (SiO_2) or quartz (Muhs 2004), but mature sand dunes in volcanic terrain settings are devoid of silica and contain minerals resistant to weathering mainly varieties of pyroxenes and some other silicate minerals as sand constituents (Craddock 2011) and as reported in this study.

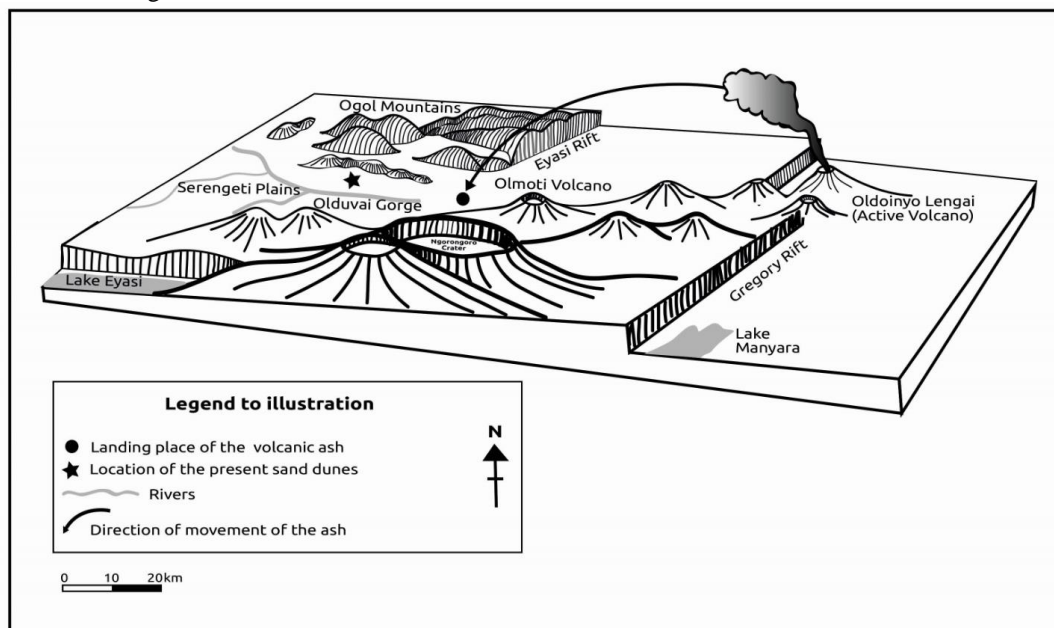


Figure 7: An artistic impression of the emplacement of the Olduvai Gorge sand dunes indicating an erupting Oldoinyo Lengai volcano located 100 km east; wind direction and volcanic ash fall in the Serengeti Plains (modified after Kafumu 2000 and Žaba and Gaidzik 2011).

Conclusions

This study presents for the first time the geochemical and mineralogical compositions (pyroxenes and some other silicates) of the Olduvai Gorge sand dunes. The geochemical composition is similar to the composition of some rock units at the Oldoinyo Lengai volcano, suggesting that the sand dunes were

derived from the Oldoinyo Lengai volcanic eruption. During the Holocene, the Oldoinyo Lengai volcanic eruption produced black ashes (tephra), which were blown westward by the prevailing wind into the nearby plains and started to migrate westward across the Serengeti Plain. Winds have reworked and accumulated the volcanic ashes into several

black sand dunes that are today referred to as “shifting sands” of the Olduvai Gorge area, serving as a geo-touristic attraction.

Acknowledgements

I thank the Free University of Brussels for funding the visit to the Olduvai Gorge and providing laboratory facilities for analysis of the sand dunes.

References

- Africantourer 2020 Olduvai Gorge shifting sands. (Accessed at: <https://africantourer.com/attraction/shifting-sands>).
- Ashley GM and Driese SG 2000 Paleopedology and paleohydrology of a volcanoclastic paleosol interval: implications for early Pleistocene stratigraphy and paleoclimate record. Olduvai Gorge Tanzania. *J. Sed. Res.* 70: 1065-1080.
- Bell K and Simonetti A 1996 Carbonatite magmatism and plume activity: implications from the Nd, Pb and Sr isotope systematics of Oldoinyo Lengai. *J. Petrol.* 37(6): 1321-1339.
- Beverly EJ, Peppe DJ, Driese SG, Blegen N, Faith JT, Tryon CA and Stinchcomb GE 2017 Reconstruction of late Pleistocene paleoenvironments using bulk geochemistry of paleosols from the Lake Victoria region. *Front. Earth Sci.* 5: Article 93, 1-20.
- Craddock RA 2011 Aeolian processes on the terrestrial planets: Recent observations and future focus. *Progr. Phys. Geogr.* 36(1): 110-124.
- Dawson JB, Keller J and Nyamweru C 1995a Historic and recent eruptive activity of Oldoinyo Lengai. In Bell K and Keller J (ed). Carbonatite volcanism: Oldoinyo Lengai and the petrogenesis of natrocarbonatites, Springer, Berlin, Heidelberg, pp. 4-22.
- Dawson JB, Smith JV and Steele IM 1995b Petrology and mineral chemistry of plutonic igneous xenoliths from the carbonatite volcano; Oldoinyo Lengai, Tanzania. *J. Petrol.* 36(3): 797-826.
- Dean JR 2005 Practical Inductively Coupled Plasma Spectroscopy, 1st Edition. Wiley. 208 p.
- Hanby J and Bygott D 1998 Ngorongoro Conservation Area, Kibuyu Partners, Karatu, Arusha, 84 p.
- Hay RL 1968 Revised stratigraphy of Olduvai Gorge, In Bishop WW and Clark JD (eds) Background to evolution in Africa, 1st edition, University of Chicago Press, Chicago, 945 p.
- Hay RL 1976 Geology of Olduvai Gorge: The study of sedimentation in a semi-arid basin, University of California Press, Chicago, 203 p.
- Kafumu DP 2000 *The quaternary stratigraphy and environments of Olduvai Gorge-Tanzania: based on fossil and related dating*. Ph.D. Thesis, Free University of Brussels, Belgium, 413 p.
- Leakey D and Roe D 1995 Olduvai Gorge, Volume 5. Excavations in Bed III, IV and the Masek Beds, 1968-1971: Cambridge University Press, Cambridge, 341 p.
- Macheyeki AS 2008 *Fault segmentation, paleostress and paleoseismic investigation in the Dodoma Area, Tanzania: Implications for seismic hazard evaluation*. Ph.D. Thesis, Ghent State University, Belgium, 342 p.
- Mollet GF and Swisher CC 2012 The Ngorongoro Volcanic Highland and its relationships to volcanic deposits at Olduvai Gorge and East African Rift volcanism. *J. Hum. Evol.* 63(2): 274-283.
- Muhs DR 2004 Mineralogical maturity in dunefields of North America, Africa and Australia. *Geomorphol.* 59: 247-269.
- Nyblade AA and Brazier R 2002 Precambrian lithospheric controls on the development of the East African rift system. *Geol.* 30(8): 755-758.
- Pickering R 1994 Ngorongoro’s geological history. Ngorongoro Conservation Area Authority, Arusha, 52 p.

- Potts PJ 1987 A handbook of Silicate Rock Analysis. Springer, Berlin, Heidelberg, 622 p.
- Roger S 2018 Geology of National Parks of Central/Southern Kenya and Northern Tanzania: Geotourism of the Gregory Rift Valley, Active Volcanism and Regional Plateaus. Springer, Berlin, Heidelberg, 256 p.
- Shackleton RM 1978 Structural development of Eastern African Rift system. In Bishop WW (ed) Geological background to fossil man: Recent researches in the Gregory Rift Valley of Eastern Africa, Scottish Academic Press 1978, London, pp. 7-15.
- Sherrod DR, Magigita MM and Kwelwa S 2013 Geologic map of Oldonyo Lengai (Oldoinyo Lengai) and surroundings, Arusha Region, United Republic of Tanzania: U.S. Geological Survey Open-File Report 2013-1306, pamphlet 65 p.
- Žaba J and Gaidzik K 2011 The Ngorongoro Crater as the biggest geotouristic attraction of the Gregory Rift (Northern Tanzania, Africa)—geological heritage. *Geotourism* 1–2 (24–25), 27-46.

APPENDIX:

Scanning electron microscopy (SEM) analysis of some mineral grains (augite, omphacite, fassaite and sillimanite)

A: Augite (Ca, Na)(Mg,Fe, Al, Ti)(Si,Al)₂O₆

Element	k-ratio (calc.)	ZAF	Atoms%	Element wt.%	wt.% err. ($\pm 1\sigma$)	No. of cations
O - K	0.0908	4.020	55.25	36.49	± 0.34	-----
Na - K	0.0029	2.753	0.85	0.80	± 0.09	1.367
Mg - K	0.0139	1.930	2.68	2.69	± 0.05	1.166
Al - K	0.0307	1.625	4.48	4.99	± 0.11	1.947
Br - L	0.0411	1.533	1.91	6.31	± 0.43	0.830
Si - K	0.1709	1.561	23.00	26.67	± 0.16	9.991
P - K	0.0047	1.836	0.67	0.86	± 0.04	0.291
Cl - K	0.0023	1.407	0.22	0.32	± 0.03	0.096
K - K	0.0136	1.204	1.01	1.64	± 0.03	0.440
Ca - K	0.0779	1.148	5.40	8.94	± 0.07	2.347
Ti - K	0.0051	1.222	0.32	0.62	± 0.07	1.137
Mn - K	0.0038	1.208	0.20	0.46	± 0.06	0.087
Fe - K	0.0782	1.178	4.00	9.21	± 0.18	1.736
Total			100.00	100.00		19.436

B: Omphacite (Ca, Na)(Mg, Fe²⁺, Al)Si₂O₆

Element	k-ratio (calc.)	ZAF	Atoms%	Element wt.%	wt.% err. ($\pm 1\sigma$)	No. of cations
O - K	0.1011	3.548	52.89	35.86	± 0.41	---
Na - K	0.0130	2.877	3.83	3.73	± 0.14	1.739
Mg - K	0.0139	2.096	2.83	2.92	± 0.08	1.284
Al - K	0.0416	1.736	6.32	7.22	± 0.16	2.867
Si - K	0.1779	1.540	23.02	27.40	± 0.17	10.448
K - K	0.0132	1.199	0.96	1.59	± 0.08	0.435
Ca - K	0.0580	1.143	3.90	6.63	± 0.07	1.770
Ti - K	0.0074	1.210	0.44	0.90	± 0.09	0.201
Mn - K	0.0035	1.213	0.18	0.43	± 0.07	0.084
Fe - K	0.1124	1.185	5.63	13.32	± 0.27	2.554
Total			100.00	100.00		21.381

C: Sillimanite (Al₂SiO₅)O

Element	k-ratio (calc.)	ZAF	Atoms%	Element wt.%	wt.% err. ($\pm 1\sigma$)	No. of cations
O – K	0.1890	2.862	67.74	54.10	± 0.51	---
Mg – K	0.0039	1.796	0.58	0.70	± 0.10	0.205
Si – K	0.3164	1.308	29.50	41.37	± 0.19	10.454
Cl – K	0.0013	1.469	0.11	0.20	± 0.03	0.039
K – K	0.0046	1.269	0.30	0.58	± 0.04	0.106
Ca – K	0.0060	1.196	0.36	0.72	± 0.04	0.127
Fe – K	0.0068	1.224	0.30	0.82	± 0.13	0.105
Al – K	0.0101	1.494	1.12	1.51	± 0.06	0.397
Total			100.00	100.00		11.432

D: Fassaite (Ca,Na)(Mg,Fe²⁺,Al,Fe³⁺,Ti)[(Si,Al)₂O₆]

Element	k-ratio (calc.)	ZAF	Atoms%	Element wt.%	wt.% err. ($\pm 1\sigma$)	No. of cations
O – K	0.2054	2.874	72.40	59.04	± 0.39	---
Na – K	0.0021	2.764	0.50	0.58	± 0.10	0.165
Mg – K	0.0174	1.933	2.71	3.36	± 0.09	0.899
Al – K	0.0512	1.657	6.17	8.49	± 0.11	2.046
Si – K	0.1330	1.528	14.20	20.33	± 0.12	4.707
P – K	0.0047	1.719	0.51	0.81	± 0.07	0.170
Cl – K	0.0018	1.379	0.13	0.24	± 0.04	0.045
K – K	0.0108	1.218	0.66	1.31	± 0.05	0.218
Ca – K	0.0396	1.169	2.27	4.63	± 0.07	0.751
Ti – K	0.0021	1.253	0.11	0.27	± 0.04	0.036
Fe – K	0.0076	1.225	1.33	0.94	± 0.07	0.109
Total			100.00	100.00		9.147

Note: The terms in scanning electron microscope (SEM) analyses: *K* = the ratio of intensity (number of X-ray counts) in the filtered peak for an element of interest in the sample to the intensity in the filtered peak for the standard assigned to that element; *k-ratio (calc.)* = *K* ratio calculation method; *ZAF* = a correction factor to convert apparent concentrations (raw peak intensity into semi quantitative concentrations) corrected for inter-element matrix effect, where *Z* stands for *atomic number*, *A* for *absorption effect* and *F* for *fluorescence effect*; *wt.* = weight; *err.* = error; and 1σ = one standard deviation.